

M uon transverse polarization in the K_{l2} process with in the SM and three Higgs doublets Weinberg model

Braguta V.V.^y, Likhoded A.A.^{yy}, Chalov A.E.^y

^y Moscow Institute of Physics and Technology, Moscow, 141700 Russia

^{yy} Institute for High Energy Physics, Protvino, 142284 Russia

Abstract

We consider two possible sources of the T -violating muon transverse polarization in the process $K^+ \rightarrow l^+ l^-$: electromagnetical state interaction in the SM and contribution due to charged Higgs exchange diagrams in the framework of the Weinberg three doublets model. It is shown that at the one-loop level of the SM the muon transverse polarization, P_T^{SM} , varies within $(0.0 \dots 1.3 \cdot 10^3)$ in the Dalitz plot region. Averaged value of the muon polarization, hP_T^{SM} is, in the kinematic region of $E \approx 20$ MeV is equal to $5.44 \cdot 10^4$. For the case of the model with three Higgs doublets the muon transverse polarization is calculated as a function of charged Higgs masses, imaginary part of the Yukawa coupling constants product and vacuum expectation values of the Higgs doublets. It is shown that the typical value of the transverse polarization in the Weinberg model is an order of magnitude smaller than that one in the SM, and its averaged value is $hP_T^{H\text{iggs}}$ is $= 4.3 \cdot 10^5$. Perspectives to probe the effect caused by the charged Higgs exchange diagrams in planned experiments are discussed.

1 Introduction

The study of the radiative $K \rightarrow m$ meson decays is extremely interesting from the point of view of searching for the new physics effects beyond the Standard Model (SM). One of the most appealing possibilities is to search for new interactions, which could lead to CP-violation. Contrary to SM, where the CP-violation is caused by the presence of the complex phase in the CKM matrix, the CP-violation in extended models, for instance, in models with three and more Higgs doublets can naturally arise due to the complex couplings of new Higgs bosons to fermions [1]. Such effects can be probed in experimental observables, which are essentially sensitive to T-odd contributions. These observables, for instance, are T-odd correlation ($T = \frac{1}{M_K^3} \mathbf{p}_K \cdot [\mathbf{p}_0 \mathbf{p}_1]$) in $K \rightarrow \pi^0 \gamma$ decay [2] and muon transverse polarization in $K \rightarrow \pi \gamma$ one. The search for new physics effects using the T-odd correlation analysis in the $K \rightarrow \pi^0 \gamma$ decay will be done in the proposed OKA experiment [3], where the statistics of 7.0 $\times 10^3$ events for the $K^+ \rightarrow \pi^0 \gamma$ decay is expected.

At the moment the E246 experiment at KEK [4] performs the $K \rightarrow \pi \gamma$ data analysis searching for T-violating muon transverse polarization. It should be noted that expected value of new physics contribution to the P_T can be of the order of $7.0 \times 10^3 \times 6.0 \times 10^2$ [5,6], depending on the extended model type. Thus, looking for the new physics effects in the muon transverse polarization it is extremely important to estimate the contribution from so called "fake" polarization, which is caused by the SM electromagnetic final state interactions and which is natural background for new interaction contributions.

The Weinberg model with three Higgs doublets [1,6] is especially interesting for the search of possible T-violation. This model allows one to have complex Yukawa couplings that leads to extremely interesting phenomenology. It was shown [2] that the study of the T-odd correlation in the $K^+ \rightarrow \pi^0 \gamma$ process allows one either to probe the terms, which are linear in CP-violating couplings, or put the strict bounds on the Weinberg model parameters. So, it seems important to analyze possible effects, which this model can induce in the muon transverse polarization in the $K \rightarrow \pi \gamma$ decay, as well.

In this paper we investigate two possible sources of the muon transverse polarization in the $K \rightarrow \pi \gamma$ process:) the effect, induced by the electromagnetic final state interaction in the one-loop approximation of the minimal quantum Electrodynamics,) the effect, induced by the charged-Higgs exchange within the three-doublets Weinberg model.

In next Section we present the calculations of the muon transverse polarization with account for one-loop diagrams with final state interactions within the SM. In Section 3 we calculate the muon transverse polarization caused by the diagrams with charged-Higgs exchange, where new charged Higgs bosons have complex couplings to fermions. Last Section summarizes the results and conclusions.

2 Muon transverse polarization in the $K^+ \rightarrow \pi^+ \gamma$ process within SM

The $K^+ \rightarrow \pi^+ \gamma$ decay in the tree level of SM is described by the diagrams shown in Fig. 1. The diagrams in Fig. 1b and 1c correspond to the muon and kaon bremsstrahlung, while the diagram in Fig. 1a corresponds to the structure radiation. This decay amplitude can be

written as follows

$$M = \frac{iep}{2} V_{us}^* f_K m \bar{u}(p) (1 + \gamma_5) \frac{p_K}{(p_K q)} \frac{(p)}{(p q)} \frac{q}{2(p q)} v(p) G 1 \quad ! \quad (1)$$

where

$$1 = \bar{u}(p) (1 + \gamma_5) v(p) \\ G = iF_v^* q(p_K) F_a (g(p_K q) p_K q) \quad (2)$$

G_F is the Fermi constant, V_{us} is the corresponding element of the CKM matrix; f_K is the K meson leptonic constant; p_K , p , p , q are the kaon, muon, neutrino, and photon four-momenta, correspondingly; * is the photon polarization vector; F_v and F_a are the kaon vector and axial form factors.

The part of the amplitude, which corresponds to the structure radiation and kaon bremsstrahlung and which will be used further in one-loop calculations, has the form :

$$M_K = \frac{iep}{2} V_{us}^* f_K m \bar{u}(p) (1 + \gamma_5) \frac{p_K}{(p_K q)} \frac{v(p)}{m} G 1 \quad ! \quad (3)$$

The partial width of the $K^+ \rightarrow \pi^+ \gamma$ decay in the K meson rest frame can be expressed as

$$d = \frac{p}{2m_K} \frac{M^2}{(2)^4} (p_K p q p) \frac{d^3 q}{(2)^3 2E_q} \frac{d^3 p}{(2)^3 2E} \frac{d^3 p}{(2)^3 2E}; \quad (4)$$

where summation over muon and photon spin states is performed.

Introducing the unit vector along the muon spin direction in muon rest frame, s , where e_i ($i = L; N; T$) are unit vectors along longitudinal, normal and transverse components of muon polarization, one can write down the squared matrix element of the transition into the particular muon polarization state in the following form :

$$M^2 = \rho [1 + (P_L e_L + P_N e_N + P_T e_T) \cdot s]; \quad (5)$$

where ρ is the Dalitz plot probability density averaged over polarization states. The e_i unit vectors can be expressed in term of three-momenta of final particles:

$$e_L = \frac{p}{p_j} \quad e_N = \frac{p}{p} \frac{(q - p)}{(q - p)j} \quad e_T = \frac{q - p}{q - p_j}; \quad (6)$$

With such definition of e_i vectors, P_T , P_L , and P_N denote transverse, longitudinal, and normal components of the muon polarization correspondingly. It is convenient to use the following variables

$$x = \frac{2E}{m_K} \quad y = \frac{2E}{m_K} = \frac{x + y}{x} \quad 1 - r \quad r = \frac{m^2}{m_K^2}; \quad (7)$$

where E and E are the photon and muon energies in the kaon rest frame. Then, the Dalitz plot probability density, as a function of the x and y variables, has the form :

$$\rho = \frac{1}{2} e^2 G_F^2 |V_{us}|^2 \frac{4m^2 f_K^2}{x^2} (1 - r) x^2 + 2(1 - r)(1 - x - \frac{r}{x})$$

$$\begin{aligned}
& + m_K^6 x^2 (F_a \vec{f} + F_v \vec{f}) (y - 2y - x + 2^2) \\
& + 4 \operatorname{Re}(f_K F_v) m_K^4 r \frac{x}{(- 1)} \\
& + 4 \operatorname{Re}(f_K F_a) m_K^4 r (- 2y + x + 2 \frac{r}{-} - \frac{x}{+} + 2) \\
& + 2 \operatorname{Re}(F_a F_v) m_K^6 x^2 (y - 2 + x)
\end{aligned} \tag{8}$$

Calculating the muon transverse polarization P_T we follow the original work [7] and assume that the amplitude of the decay is CP-invariant, and the f_K , F_v , and F_a form factors are real. In this case the tree level muon polarization $P_T = 0$. When one-loop contributions are incorporated, the nonvanishing muon transverse polarization can arise due to the interference of tree-level diagrams and imaginary parts of one-loop diagrams, induced by the electromagnetic state interaction.

To calculate form factor imaginary parts one can use the S-matrix unitarity:

$$S^+ S = 1 \tag{9}$$

and, using $S = 1 + iT$, one gets:

$$T_{fi} - T_{if} = i \sum_n^X T_{nf} T_{ni}; \tag{10}$$

where i ; f ; n indices correspond to the initial, final, and intermediate states of the particle system. Further, using the T -invariance of the M matrix element one gets:

$$\operatorname{Im} T_{fi} = \frac{1}{2} \sum_n^X T_{nf} T_{ni} \tag{11}$$

$$T_{fi} = (2)^4 (P_f - P_i) M_{fi} \tag{12}$$

SM one-loop diagrams, which contribute to the muon transverse polarization in the $K^+ \pi^+$ decay, are shown in Fig. 2. Using Eq. (3) one can write down imaginary parts of these diagrams. For diagrams in Figs. 2a, 2c one has

$$\begin{aligned}
\operatorname{Im} M_1 = & \frac{ie}{2} \frac{G_F}{2} V_{us} \bar{u}(p) (1 + \gamma_5) \int^Z \frac{d^3 k}{2!} \frac{d^3 k}{2!} (k + k - P) R \\
& (\hat{k} - m) \frac{\hat{q} + \hat{p}}{(q + p)^2} \frac{m}{m^2} " v(p)
\end{aligned} \tag{13}$$

For diagrams in Figs. 2b, 2d one has

$$\begin{aligned}
\operatorname{Im} M_2 = & \frac{ie}{2} \frac{G_F}{2} V_{us} \bar{u}(p) (1 + \gamma_5) \int^Z \frac{d^3 k}{2!} \frac{d^3 k}{2!} (k + k - P) R \\
& (\hat{k} - m) " \frac{\hat{k}}{(k - q)^2} \frac{\hat{q} - m}{m^2} v(p);
\end{aligned} \tag{14}$$

where

$$\begin{aligned}
R = & f_K m \frac{(p_K)}{(p_K k)} \frac{1}{m} - i F_v " (k) (p_K) \\
& + F_a (- (p_K k) - (p_K) \hat{k}):
\end{aligned} \tag{15}$$

To write down the contributions from diagrams in Figs. 2e, 2f, R should be substituted by

$$R = f_K m \frac{1}{m} \frac{(k_1)}{(k_1 k_2)} \frac{\hat{k}}{2(k_1 k_2)} \quad (16)$$

in expressions (13), (14).

We do not present the expression for the imaginary part of the diagram in Fig. 2g and further, in calculations, we neglect this diagram contribution to muon transverse polarization, because, as it will be shown later, its contribution is negligibly small in comparison with the contribution from other diagrams.

The details of the integrals calculation entering Eqs. (13), (14), and their dependence on kinematical parameters are given in Appendix 1.

The expression for the amplitude with account for imaginary one-loop contributions can be written as:

$$M = \frac{iep}{2} V_{us}'' f_K m \bar{u}(p) (1 + \frac{p_K}{q}) \frac{p_K}{(p_K q)} \frac{(p)}{(p q)} v(p) + \\ F_n \bar{u}(p) (1 + \frac{p}{q}) \hat{q} v(p) \quad G = 1; \quad (17)$$

where

$$G = iF_v'' q(p_K) F_a(q(p_K q) p_K q); \quad (18)$$

The f_K ; F_v ; F_a , and F_n form factors include one-loop contributions from diagrams shown in Figs. 2a-2f. The choice of the form factors is determined by the matrix element expansion into set of gauge-invariant structures.

As far as we are interested in the contributions of imaginary parts of one-loop diagrams only, since namely they lead to nonvanishing transverse polarization, we neglect the real parts of these diagrams and assume that $Re f_K$; $Re F_v$; $Re F_a$ coincide with their tree-level values, f_K ; F_v ; F_a , correspondingly, and $Re F_n = f_K m = 2(p q)$. Explicit expressions for imaginary parts of the form factors are given in Appendix 2.

The muon transverse polarization can be written as

$$P_T = \frac{T}{0}; \quad (19)$$

where

$$T = 2m_K^3 e^2 G_F^2 \bar{u}^2 x \frac{q}{y^2 - r} m \text{Im} (f_K F_a) (1 - \frac{2}{x} + \frac{y}{x}) \\ + m \text{Im} (f_K F_v) (\frac{y}{x} - 1 - 2\frac{r}{x}) + 2\frac{r}{x} \text{Im} (f_K F_n) (1 - \frac{r}{x}) \\ + m_K^2 x \text{Im} (F_n F_a) (-1) + m_K^2 x \text{Im} (F_n F_v) (-1) \quad (20)$$

It should be noted that our expression for the Dalitz plot probability density, ρ , differs from that one obtained in earlier papers [15,16] by the structure of interference terms. Besides, expression (20) also disagrees with T in [15,16]. In particular, the terms containing

$\text{Im } F_n$ are missed in the T expression given in [15,16], and the $\text{Im } (f_K F_a)$ term has the opposite sign. Moreover, calculating the muon transverse polarization we took into account the diagrams shown in Fig. 2e and 2f, which have been neglected in [15], and which give the contribution comparable with the contribution from other diagrams in Fig. 2. It should be noted, that ϕ was also calculated in [13], and, though, all the kinematical structures coincide with ours, except for the terms $\text{Re}(f_K F_v)$ and $\text{Re}(F_a F_v)$, which have the opposite sign.

3 Three Higgs doublets Weinberg model

As it was shown in original paper by Weinberg [1], one of possible sources of spontaneous CP-violation due to the charged-Higgs bosons exchange is the presence of different relative phases of vacuum expectation values of Higgs doublets. However, the Natural Flavor Conservation requires at least three Higgs doublets. In the framework of this model there are three sources of CP-violation:

- (I) the complex CKM matrix;
- (II) a phase in the charged-Higgs boson mixing;
- (III) neutral scalar-pseudoscalar mixing.

In the original Weinberg three-Higgs-doublet model, CP is broken spontaneously, CKM-matrix is real, and observed CP-violation in the neutral kaon sector comes solely from charged-Higgs boson exchange. However, as it was shown in [9], in the framework of this model the charged and neutral Higgs boson exchange can lead to the noticeable effect in the NEDM value, while the transverse muon polarization in the $K^+ \rightarrow \pi^+ \nu \bar{\nu}$ decay is affected by the charged-Higgs boson exchange only. So, to single out the effect (II), we will suppose, following the ideology of [6], that CP-violation effect due to the neutral Higgs boson exchange is smaller than that one caused by the charged-Higgs boson exchange.

In the framework of the Weinberg model the charged Higgs boson interaction with quarks and leptons and be represented as:

$$L_Y = (2 \frac{p}{2G_F})^{1/2} \sum_{i=1}^{X^2} (i U_L K M_D D_R + i U_R M_U K D_L + i N_L M_E E_R) H_i^+ + H.C.;$$

where K is the CKM matrix, M_U ; M_D ; M_E are the mass matrices for quarks of d- and u-type and charged leptons, correspondingly; i ; i ; i are the complex couplings, which are interrelated as follows [10]

$$\frac{\text{Im } (i_{22})}{\text{Im } (i_{11})} = \frac{\text{Im } (i_{22})}{\text{Im } (i_{11})} = \frac{\text{Im } (i_{22})}{\text{Im } (i_{11})} = -1$$

and

$$\frac{1}{v_2^2} \text{Im } (i_{11}) = \frac{1}{v_1^2} \text{Im } (i_{11}) = \frac{1}{v_3^2} \text{Im } (i_{11})$$

where v_i ($i = 1, 2, 3$) are the vacuum expectation values of Higgs doublets, v_i , and

$$v = (v_1^2 + v_2^2 + v_3^2)^{1/2} = (2 \frac{p}{2G_F})^{1/2}$$

In the model with three Higgs doublets the $K^+ \rightarrow \pi^+ \nu \bar{\nu}$ decay amplitude can be written as:

$$M = M_{SM} + M_{Higgs};$$

where M_{SM} is the SM part of the amplitude with W -boson exchange, and M_{Higgs} is the part amplitude due to the charged-Higgs boson exchange. The amplitude due to charged-Higgs boson exchange is

$$M_{Higgs} = \frac{e p_F}{2} V_{us} [h \bar{s}_5 u \bar{K}^+ i^- (1 + \gamma_5) + h_0 \bar{s}_5 u \bar{K}^+ i^- (1 + \gamma_5) \frac{\hat{p} \cdot \hat{q} + m}{2(p \cdot q)} \mathbf{u} \cdot \mathbf{J};$$

where

$$J = m \sum_{i=1}^{x^2} \frac{m_u \gamma_i \gamma_i m_s \gamma_i \gamma_i}{M_{H_i}^2} :$$

The amplitude gets the contributions from the $h_0 \bar{s}_5 u \bar{K}^+ i^-$ and $h \bar{s}_5 u \bar{K}^+ i^-$ matrix elements, which can be expressed in terms of the f_K form factor, using its definition and requiring the gauge invariance of the matrix element:

$$h_0 \bar{s}_5 u \bar{K}^+ i^- = i \frac{m_K^2 f_K}{m_s + m_u}$$

$$h \bar{s}_5 u \bar{K}^+ i^- = i \frac{m_K^2 f_K}{(m_s + m_u)(p_K \cdot q)} (p_K \cdot \mathbf{u})$$

From now on, to simplify the expressions, we introduce the following constant:

$$= \frac{m_K^2 f_K}{m_s + m_u}$$

Using this notation one can rewrite the total amplitude as follows

$$M = i e p_F \frac{G_F}{2} V_{us}'' (f_K m \gamma J) \bar{u}(p) (1 + \gamma_5)$$

$$= \frac{p_K}{(p_K \cdot q)} \frac{(p \cdot \mathbf{u})}{(p \cdot q)} \frac{\hat{q}}{2(p \cdot q)} v(p) G \gamma$$

Then γ_0 takes the form :

$$\gamma_0 = \frac{1}{2} e^2 G_F^2 V_{us}^2 \frac{4(m_K f_K \gamma J)^2}{x^2} (1 - x^2 + 2(1 - r)(1 - x - \frac{r}{x}) +$$

$$+ m_K^6 x^2 (F_a^2 + F_v^2) (y - 2y - x + 2r^2) +$$

$$+ 4(f_K F_v - \frac{F_v \text{Re}(J)}{m_K}) m_K^4 r \frac{x}{x - 1} +$$

$$+ 4(f_K F_a - \frac{F_a \text{Re}(J)}{m_K}) m_K^4 r (-2y + x + 2\frac{r}{x} - \frac{x}{x - 2}) +$$

$$+ 2(F_a F_v) m_K^6 x^2 (y - 2 + x)$$

The muon transverse polarization is $P_T = \tau = 0$, where

$$\tau = \frac{2m_K^3 e^2 G_F^2 J_{us}^2 \text{Im}(J)}{q \frac{y^2}{y^2 - r} 2xF_v + 2F_a + \frac{1}{(2r F_v)(x + y)(F_a + F_v))}}$$

and¹

$$\text{Im}(J) = m_s \frac{\text{Im}(\Gamma_{11}) v_2^2}{M_H^2 v_3^2} : \quad (21)$$

Thus, the value of muon transverse polarization in the framework of this model is the function of charged-Higgs boson masses, vacuum expectation values and imaginary part of Yukawa couplings product. P_T reaches its maximal value at maximal values of $\text{Im}(\Gamma_{11})$ and $v_2^2 = v_3^2$ and at minimal mass of charged-Higgs boson. Therefore, to estimate the model effect in the muon transverse polarization one needs to know bounds on the model parameters, which follow from experimental data.

As it was pointed out in [6], the bounds on the parameters of Weinberg model can be determined from :

I. LEP II data on direct search of charged-Higgs boson. The current bound [11] on the charged-Higgs boson mass is

$$M_H = 69 \text{ GeV} : \quad (22)$$

II. Model bounds for the analog of the CKM matrix for the charged-Higgs boson mixing, which relates vacuum expectation values of Higgs doublets [6]:

$$\frac{q \frac{v_3}{v_1^2 + v_2^2 + v_3^2}}{2v_1 v_2} = 9 : \quad (23)$$

III. Bounds on the $v_2 = v_1$ ratio from the $D^0 - \bar{D}^0$ -mixing data. Dominant contribution to the D -meson mass difference, M_D , due to the $D^0 - \bar{D}^0$ -mixing and caused by box-diagram with charged-Higgs bosons, can be written as

$$M_D = \frac{G_F^2}{24^2} \sin^2 \theta_W f_D^2 B_D \frac{m_s^4}{M_H^2} \left(\frac{v_2}{v_1}\right)^4 : \quad (24)$$

IV. Bounds coming from the experimental data on neutron electric dipole moment (NEDM). At one-loop level, taking into account diagrams with charged-Higgs boson exchange, one can write down the expression for NEDM as follows [12]:

$$d_n = \frac{4}{3} d_a = -\frac{2G_F}{9^2} m_d \text{Im}(\Gamma_{11}) \sum_{i=\text{ct}}^p \frac{x_i}{(1-x_i)^2} \left(\frac{5}{4} x_i - \frac{3}{4} \right) \frac{1}{1-x_i} \ln \frac{3x_i}{2x_i} K_{id}^2 ; \quad (25)$$

$$x_i = m_i^2 = M_H^2 .$$

In Figs. 3a-3c we present the allowed parameter regions, which follow from (22)-(25). Further, calculating the muon transverse polarization in the framework of the Weinberg model we will adopt the model parameters taking into account the bounds above.

¹Here and further we assume that $M_{H_2} \gg M_{H_1} = M_H$ and neglect the term multiplied by m_u .

4 Results and discussion

For the numerical calculations we use the following form factor values

$$f_K = 0.16 \text{ GeV}; F_V = \frac{0.095}{m_K}; F_A = \frac{0.043}{m_K} :$$

The f_K form factor is determined from experimental data on kaon decays [11], and F_V, F_A ones are calculated at the one loop-level in the Chiral Perturbation Theory [13]. With these choice of form factor values the decay branching with the cut on photon energy $E > 20 \text{ MeV}$ is equal to $\text{Br}(K^+ \rightarrow e^+ \gamma) = 3.3 \cdot 10^3$, and with the cut on muon momentum $|\vec{p}_\mu| < 231.5 \text{ MeV}/$ is equal to $\text{Br}(K^+ \rightarrow e^+ \gamma) = 6.2 \cdot 10^3$, that is in good agreement with PDG data.

The Standard Model case

The three-dimensional distribution of muon transverse polarization, calculated at the SM one-loop approximation is shown in Fig. 4. It should be noted that P_T as the function of the x and y parameters is characterized by the sum of individual contributions of diagrams in Figs. 2a-f, while the contributions from diagrams 2a-d [8] and 2e-f are comparable in absolute value, but opposite in sign, so the total $P_T(x; y)$ distribution is the difference of these group contributions and in absolute value is about one order of magnitude less than each of them. Our estimates show that in the Dalitz plot region the contribution from diagram 2g is an order of magnitude less than the total contribution from other diagrams.

As one can see in Fig. 4, the maximal absolute value of the muon transverse polarization is achieved in two domains of the Dalitz plot region:

- a) at $0.2 \leq x = 2E/m_K \leq 0.4$ and $y = 2E/m_K \approx 1$;
- b) at $0.4 \leq x = 2E/m_K \leq 0.7$ and $0.5 \leq y = 2E/m_K \leq 0.7$.

Indeed, analysing the level lines for P_T , shown in Fig. 5, it is easy to notice that the maximal values of P_T are located near to the $x; y$ values $(0.3; 1.0)$ and $(0.6; 0.6)$. It should be noted that the value of muon transverse polarization is negative in the whole Dalitz plot region and does not take positive values. Averaged value of transverse polarization can be obtained by integrating the function $P_T = \langle K^+ \rightarrow e^+ \gamma \rangle$ over the physical region, and with the cut on photon energy $E > 20 \text{ MeV}$ it is equal to

$$\langle P_T \rangle = 5.44 \cdot 10^4 : \quad (26)$$

Let us note that obtained numerical value of the averaged transverse polarization and $P_T(x; y)$ kinematical dependence in Dalitz plot differ from those given in [15-17]. As it was calculated in [15], the P_T value varies in the region of $(-0.1 \dots 4.0) \cdot 10^3$ for cuts on the muon and photon energies, $200 < E < 254.5 \text{ MeV}$, $20 < E < 200 \text{ MeV}$. We have already mentioned above that

- 1) The authors of [15] did not take into account terms containing the imaginary part of the F_n form factor (contributing to P_T), which are, in general, not small being compared with others.
- 2) In our expression for P_T (see (20)) the $\text{Im}(f_K F_A)$ term has the opposite sign.
- 3) The $x; y$ -dependence of the structures at interference terms in expression for P_T disagrees with our results.

4) The authors of [15] omitted the diagrams, shown in Fig. 2e, 2f, though, as it was mentioned above, their contribution to P_T is comparable with that one of diagrams in Fig. 2a-2d.

All these points lead to serious disagreement between our results and results obtained in [15]. In particular, our calculations show that the value of the muon transverse polarization has negative sign in all Dalitz plot region and its absolute value varies in the region of $(0.0 \dots 1.3) \times 10^3$, and the P_T dependence on the $x; y$ parameters is different than in [15].

We would like to remark that the muon transverse polarization for the same process was also calculated in [17]. However, the calculation method used in [17] does not allow to compare the analytical results, but as for the numerical ones, they differ from our results and results of [15] as well: though the P_T value is negative in whole physical region (that agrees with our results), its absolute values does not exceed 4×10^4 and the $P_T(x; y)$ distribution is essentially different. The absence of the explicit expressions for ϕ_0 and ϕ_T functions and imaginary parts of form factors excludes the possibility to compare results [17] with the results by other authors.

W einberg model case

Calculating the muon transverse polarization within the three doublet model we choose the model parameters in a way, first, to maximize the polarization value and, second, to satisfy the bounds of (22)–(25). In Fig. 6 we present the three-dimensional P_T distribution for the Weinberg model case with $M_H = 70$ GeV, $\text{Im}(J) = 7 \times 10^5$, and kinematical cut $E > 20$ MeV.

The behaviour of the transverse polarization as the function $P_T^{\text{Higgs}} = f(x; y)$ in the case of the three doublet model is significantly different from that one in SM. First, in this model the sign of the transverse polarization depends on the sign of $\text{Im}(J)$, see (21). Second, the $P_T^{\text{Higgs}} = f(x; y)$ function has different behaviour and the region of maximal absolute values is located in different $(x; y)$ region: $0.65 \leq x \leq 0.75$ and $0.75 \leq y \leq 0.85$. Corresponding level lines $P_T^{\text{Higgs}} = f(x; y)$ are shown in Fig. 7.

Comparing the P_T distributions in the case of SM and Weinberg model, Figs. 4 and 6, one can see that the maximal value of the transverse polarization in the case of the Weinberg model is one order of magnitude less than that one in SM. The averaged P_T value, obtained by integrating over the Dalitz plot region with the cut $E > 20$ MeV, is

$$\langle P_T^{\text{Higgs}} \rangle = 4.3 \times 10^5; \quad (27)$$

that is again an order of magnitude less than (26). So, for reliable detection of the charged-Higgs effect one needs the experimental sensitivity to probe the transverse polarization in the K_2 process at the level of 10^{-5} . Experiments conducted thus far are sensitive to P_T at the level of 1.5×10^2 [4], that is evidently insufficient to discover the effect.

Nevertheless, there are possibilities, connected with the upgrade of the E246 experiment (expected sensitivity is about 2×10^3), and launch of new experiment E923 [14], where the usage of a new method of T-odd polarization measurement allows to achieve the level of 10^{-4} , that seems more optimistic. Moreover, comparing the $P_T = f(x; y)$ in Figs. 4–6, one can notice that the relative $P_T^{\text{Higgs}} = P_T^{\text{SM}}$ contribution can be significantly enhanced

by introducing cuts in $(x; y)$ region. The statistics increase will allow one to analyse the distribution for $P_T = f(x; y)$ rather than its average value only.

Excluding regions of small x and y , for instance, $x < 0.4$ and $y < 0.7$ one can significantly suppress the background SM contribution without a noticeable loss of the signal, induced by charged-Higgs bosons.

Acknowledgements

The authors thank Drs. Kiselev V.V. and Likhoded A.K. for fruitful discussion and valuable remarks. This work is in part supported by the Russian Foundation for Basic Research, grants 99-02-16558 and 00-15-96645, and Russian Education Ministry, grant RF E 00-33-062.

R eferences

1. S. Weinberg, Phys. Rev. Lett. 37 (1976), 651.
2. A. Likhoded, V. Braguta, A. Chalov, in press (see. also hep-ex/0011033).
3. V.F. Obratsov and L.G. Landsberg, hep-ex/0011033).
4. See, for example, Yu.G. Kudenko, hep-ex/00103007).
5. J.F. Donoghue and B. Holstein, Phys. Lett. B 113 (1982), 382; L.W. olenstein, Phys. Rev. 29 (1984), 2130; G. Barenboim et al., Phys. Rev. 55 (1997), 24213; M. Kobayashi, T.-T. Lin, Y. Okada, Prog. Theor. Phys. 95 (1996), 361; S.S. Gershtein et al., Z. Phys. C 24 (1984), 305; R. Garisto, G. Kane, Phys. Rev. D 44 (1991), 2038.
6. G. Belanger, C.Q. Geng, Phys. Rev. D 44 (1991), 2789.
7. L.B. Okun and I.B. Khriplovich, Sov. Journ. Nucl. Phys. v.6 (1967), 821.
8. A. Likhoded, V. Braguta, A. Chalov, Preprint IHEP 2000-57, 2000; to appear in Phys. Atom. Nucl.
9. A.R. Zhitnitskii, Sov. J. Nucl. Phys., 31 (1980), 529; ., C.Q. Geng and J.N. Ng, Phys. Rev. D 42 (1990), 1509.
10. H.Y. Cheng, Phys. Rev. D 26 (1982), 143.
11. Review of Particle Physics, Euro. Phys. Journ. C 15 (2000).
12. G. Beal and N.G. Deshpande, Phys. Lett. B 132 (1983), 427.
13. J. Bijnens, G. Ecker, J. Gasser, Nucl. Phys. B 396 (1993), 81.
14. M.V. Diwan et al., AGS Experiment Proposal 923, 1996.
15. V.P. Frolov, Yu.G. Kudenko, Phys. Atom. Nucl. v.67 (1999), 1054.
16. C.H. Chen, C.Q. Geng, C.C. Lin hep-ph/9709447
17. R.N. Rogalev, Preprint IHEP 2001-5, 2001.

Appendix 1

Calculating the integrals, contributing to (14) and (15), we use the following notations:

$$P = p + q$$

$$d = \frac{d^3 k}{2!} \frac{d^3 k}{2!} (k + k - P)$$

We present below either the explicit expressions for integrals, or the set of equations, which being solved, give the parameters, entering the integrals.

$$\begin{aligned} J_{11} &= \int d = \frac{1}{2} \frac{P^2 - m_K^2}{P^2} ; \\ J_{12} &= \int d \frac{1}{(p_K k)} = \frac{1}{2I} \ln \frac{(P p_K) + I}{(P p_K) - I} ; \end{aligned}$$

where

$$\begin{aligned} I^2 &= (P p_K)^2 - m_K^2 P^2 : \\ \int d \frac{k}{(p_K k)} &= a_{11} p_K + b_{11} P : \end{aligned}$$

The a_{11} and b_{11} parameters are determined by the following equation:

$$\begin{aligned} a_{11} &= \frac{1}{(P p_K)^2 - m_K^2 P^2} P^2 J_{11} - \frac{J_{12}}{2} (P p_K) (P^2 - m^2) ; \\ b_{11} &= \frac{1}{(P p_K)^2 - m_K^2 P^2} (P p_K) J_{11} - \frac{J_{12}}{2} m_K^2 (P^2 - m^2) : \\ \int d k &= a_{12} P ; \\ \int d k k &= a_{13} g + b_{13} P P ; \end{aligned}$$

where

$$\begin{aligned} a_{12} &= \frac{(P^2 - m^2)}{2P^2} J_{11} ; \\ a_{13} &= \frac{1}{12} \frac{(P^2 - m^2)^2}{P^2} J_{11} ; \\ b_{13} &= \frac{1}{3} \frac{P^2 - m^2}{P^2} J_{11} : \\ J_1 &= \int d \frac{1}{(p_K k) ((P - k)^2 - m^2)} = \frac{1}{2I_1 (P^2 - m^2)} \ln \frac{(p_K p) + I_1}{(p_K p) - I_1} ; \\ J_2 &= \int d \frac{1}{(P - k)^2 - m^2} = \frac{1}{4I_2} \ln \frac{(P p) + I_2}{(P p) - I_2} ; \end{aligned}$$

where

$$\begin{aligned} I_1^2 &= (p_K p)^2 - m^2 m_K^2 ; \\ I_2^2 &= (P p)^2 - m^2 P^2 ; \end{aligned}$$

$$\begin{aligned} d \frac{k}{(p - k)^2 - m^2} &= a_1 P + b_1 p ; \\ a_1 &= \frac{m^2 (P^2 - m^2) J_2 + (P p) J_{11}}{2(P p)^2 - m^2 P^2} ; \\ b_1 &= \frac{(P p) (P^2 - m^2) J_2 + P^2 J_{11}}{2(P p)^2 - m^2 P^2} ; \end{aligned}$$

The integrals below are determined by the parameters, which can be obtained by solving the sets of equations.

$$\begin{aligned} d \frac{k}{(p_K k) ((p - k)^2 - m^2)} &= a_2 P + b_2 p_K + c_2 p ; \\ \stackrel{8}{\approx} a_2 (P p_K) + b_2 m_K^2 + c_2 (p_K p) &= J_2 \\ \stackrel{8}{\approx} a_2 (P p) + b_2 (p_K p) + c_2 m^2 &= \frac{1}{2} J_{12} \\ \stackrel{8}{\approx} a_2 P^2 + b_2 (P p_K) + c_2 (P p) &= (p q) J_1 \end{aligned}$$

$$\begin{aligned} d \frac{k k}{(p_K k) ((p - k)^2 - m^2)} &= a_3 g + b_3 (P p_K + P p_K) + c_3 (P p + P p) \\ &\quad + d_3 (p_K p + p_K p) + e_3 p p \\ &\quad + f_3 P P + g_3 p_K p_K ; \end{aligned}$$

$$\begin{aligned} \stackrel{8}{\approx} 4a_3 + 2b_3 (P p_K) + 2c_3 (P p) + 2d_3 (p_K p) + g_3 m_K^2 + e_3 m^2 + f_3 P^2 &= 0 \\ c_3 (p_K p) + b_3 m_K^2 + f_3 (P p_K) & a_1 = 0 \\ c_3 (P p_K) + d_3 m_K^2 + e_3 (p_K p) & b_1 = 0 \\ a_3 + b_3 (P p_K) + d_3 (p_K p) + g_3 m_K^2 &= 0 \\ b_3 (p_K p) + c_3 m^2 + f_3 (P p) &= \frac{1}{2} b_{11} \\ b_3 (P p) + d_3 m^2 + g_3 (p_K p) &= \frac{1}{2} a_{11} \\ \stackrel{8}{\approx} a_3 P^2 + 2b_3 P^2 (P p_K) + 2c_3 P^2 (P p) + 2d_3 (P p) (P p_K) + e_3 (P p)^2 + f_3 (P^2)^2 + g_3 (P p_K)^2 &= (p q)^2 J_1 \end{aligned}$$

$$\begin{aligned} d \frac{k k}{(p - k)^2 - m^2} &= a_4 g + b_4 (P p + P p) + c_4 P P + d_4 p p ; \\ \stackrel{8}{\approx} a_4 + d_4 m^2 + b_4 (P p) &= 0 \\ \stackrel{8}{\approx} b_4 m^2 + c_4 (P p) &= \frac{1}{2} a_{12} \\ \stackrel{8}{\approx} 4a_4 + 2b_4 (P p) + c_4 P^2 + d_4 m^2 &= 0 \\ \stackrel{8}{\approx} a_4 P^2 + 2b_4 P^2 (P p) + c_4 (P^2)^2 + d_4 (P p)^2 &= \frac{(P^2 - m^2)^2}{4} J_2 \end{aligned}$$

$$\begin{aligned}
d \frac{k \cdot k \cdot k}{(p \cdot k)^2 - m^2} = & a_5(g \cdot p + g \cdot p + g \cdot p) + b_5(g \cdot P + g \cdot P + g \cdot P) \\
& + c_5 p \cdot p \cdot p + d_5 P \cdot P \cdot P + e_5 (P \cdot p \cdot p + P \cdot p \cdot p + P \cdot p \cdot p) \\
& + f_5 (P \cdot P \cdot p + P \cdot P \cdot p + P \cdot P \cdot p);
\end{aligned}$$

$$\begin{aligned}
& 2a_5 + c_5 m^2 + e_5 (P \cdot p) = 0 \\
& a_5 m^2 + b_5 (P \cdot p) = \frac{1}{2} a_{13} \\
& b_5 + e_5 m^2 + f_5 (P \cdot p) = 0 \\
& d_5 (P \cdot p) + f_5 m^2 = \frac{1}{2} b_{13} \\
& 6a_5 + c_5 m^2 + 2e_5 (P \cdot p) + f_5 P^2 = 0 \\
& \vdots 3a_5 P^2 (P \cdot p) + 3b_5 (P^2)^2 + c_5 (P \cdot p)^3 + d_5 (P^2)^3 + 3e_5 P^2 (P \cdot p)^2 + 3f_5 (P^2)^2 (P \cdot p) = \frac{(P^2 - m^2)^3}{8} J_2
\end{aligned}$$

Appendix 2

Here we present the expressions for imaginary parts of form-factors as the functions of parameters, calculated in Appendix 1.

$$\begin{aligned}
 \text{Im } \tilde{f}_K &= \frac{1}{2} f_K (-4a_3(p_K q) + 4a_2 m^2 (p_K q) - 2b_3 m^2 (p_K q) + 4c_2 m^2 (p_K q) \\
 &\quad - 4c_3 m^2 (p_K q) - 2d_3 m^2 (p_K q) - 2e_3 m^2 (p_K q) - 2f_3 m^2 (p_K q) + \\
 &\quad 4a_2 (p_K q) (p q) - 4b_3 (p_K q) (p q) - 4c_3 (p_K q) (p q) - 4f_3 (p_K q) (p q)) + \\
 &\quad \frac{1}{2} F_a (8a_4 (p_K q) - 8a_5 (p_K q) - 8b_5 (p_K q) + 8b_4 m^2 (p_K q) + \\
 &\quad 4c_4 m^2 (p_K q) - 2c_5 m^2 (p_K q) + 4d_4 m^2 (p_K q) - 2d_5 m^2 (p_K q) \\
 &\quad - 6e_5 m^2 (p_K q) - 6f_5 m^2 (p_K q) + 12b_4 (p_K q) (p q) + 8c_4 (p_K q) (p q) + \\
 &\quad 4d_4 (p_K q) (p q) - 4d_5 (p_K q) (p q) - 4e_5 (p_K q) (p q) - 8f_5 (p_K q) (p q)) + \\
 &\quad \frac{1}{2} F_v (8a_4 (p_K q) - 8a_5 (p_K q) - 8b_5 (p_K q) + 8b_4 m^2 (p_K q) + \\
 &\quad 4c_4 m^2 (p_K q) - 2c_5 m^2 (p_K q) + 4d_4 m^2 (p_K q) - 2d_5 m^2 (p_K q) \\
 &\quad - 6e_5 m^2 (p_K q) - 6f_5 m^2 (p_K q) + 12b_4 (p_K q) (p q) + 8c_4 (p_K q) (p q) + \\
 &\quad 4d_4 (p_K q) (p q) - 4d_5 (p_K q) (p q) - 4e_5 (p_K q) (p q) - 8f_5 (p_K q) (p q))
 \end{aligned}$$

$$\begin{aligned}
 \text{Im } \tilde{F}_a &= \frac{1}{2} f_K (a_2 m^2 + 2 c_2 m^2 - c_3 m^2 - 2 d_3 m^2 - e_3 m^2 \\
 &\quad - \frac{a_1 m^2}{(p q)} - \frac{b_1 m^2}{(p q)} + \frac{2 b_4 m^2}{(p q)} + \frac{c_4 m^2}{(p q)} + \frac{d_4 m^2}{(p q)} + \\
 &\quad - \frac{1}{2} F_v (8 a_4 - 4 a_5 - 12 b_5 - 2 a_1 m^2 + 4 b_4 m^2 + 5 c_4 m^2 - c_5 m^2 \\
 &\quad - d_4 m^2 - 3 d_5 m^2 - 5 e_5 m^2 - 7 f_5 m^2 + 2 a_1 (p_K p) - 4 b_4 (p_K p) \\
 &\quad - 4 c_4 (p_K p) + 2 d_5 (p_K p) + 2 e_5 (p_K p) + 4 f_5 (p_K p) + 2 a_1 (p_K q) \\
 &\quad - 2 b_4 (p_K q) - 4 c_4 (p_K q) + 2 d_5 (p_K q) + 2 f_5 (p_K q) - 4 a_1 (p q) + \\
 &\quad 6 b_4 (p q) + 10 c_4 (p q) - 6 d_5 (p q) - 2 e_5 (p q) - 8 f_5 (p q)) + \\
 &\quad \frac{1}{2} F_a (-6 a_4 + 2 a_5 + c_4 m^2 - d_4 m^2 - d_5 m^2 \\
 &\quad - e_5 m^2 - 2 f_5 m^2 + 2 a_1 (p_K p) - 4 b_4 (p_K p) - 4 c_4 (p_K p) + \\
 &\quad 2 d_5 (p_K p) + 2 e_5 (p_K p) + 4 f_5 (p_K p) + 2 a_1 (p_K q) - 2 b_4 (p_K q) \\
 &\quad - 4 c_4 (p_K q) + 2 d_5 (p_K q) + 2 f_5 (p_K q) + 2 c_4 (p q) - 2 d_5 (p q) - 2 f_5 (p q))
 \end{aligned}$$

$$\begin{aligned}
\Im F_n &= \frac{1}{2} f_K \quad 4 a_1 m + 2 a_3 m + 2 b_1 m + b_{11} m \quad 2 b_4 m \quad 2 c_4 m \\
&\quad J_{12} m \quad 2 J_2 m \quad b_2 m_K^2 m + g_3 m_K^2 m \quad 2 a_2 m^3 \\
&\quad c_2 m^3 + c_3 m^3 + f_3 m^3 \quad 2 a_2 m (p_K p) \quad 2 b_2 m (p_K p) + \\
&\quad 2 b_3 m (p_K p) \quad 2 c_2 m (p_K p) + 2 d_3 m (p_K p) + 2 J_1 m (p_K p) + \\
&\quad 2 b_3 m (p_K q) \quad \frac{a_{12} m^3}{(p q)^2} \quad \frac{J_{11} m^3}{(p q)^2} \quad \frac{a_{12} m}{(p q)} \quad \frac{2 a_4 m}{(p q)} + \\
&\quad \frac{J_{11} m}{(p q)} \quad \frac{a_{11} m_K^2 m}{2 (p q)} + \frac{3 a_1 m^3}{(p q)} + \frac{3 b_1 m^3}{(p q)} + \frac{b_{11} m^3}{2 (p q)} \\
&\quad \frac{2 J_2 m^3}{(p q)} \quad \frac{b_{11} m (p_K p)}{(p q)} + \frac{J_{12} m (p_K p)}{(p q)} \quad \frac{b_{11} m (p_K q)}{(p q)} + \\
&\quad \frac{J_{12} m (p_K q)}{(p q)} \quad 2 a_2 m (p q) + 2 c_3 m (p q) + 2 f_3 m (p q) + \\
&\quad \frac{1}{2} F_v \quad 2 a_4 m \quad 4 a_5 m + 2 b_{13} m \quad 4 b_5 m \\
&\quad 2 a_1 m^3 + c_4 m^3 \quad c_5 m^3 \quad d_4 m^3 \quad d_5 m^3 \quad 3 e_5 m^3 \\
&\quad 3 f_5 m^3 + 2 a_1 m (p_K p) \quad 2 c_4 m (p_K p) + 2 d_4 m (p_K p) + \\
&\quad 2 d_5 m (p_K p) + 2 e_5 m (p_K p) + 4 f_5 m (p_K p) \quad 2 c_4 m (p_K q) + \\
&\quad 2 d_5 m (p_K q) + 2 f_5 m (p_K q) + \frac{3 a_{13} m}{(p q)} + \frac{b_{13} m^3}{(p q)} \\
&\quad \frac{b_{13} m (p_K p)}{(p q)} \quad \frac{b_{13} m (p_K q)}{(p q)} \quad 2 a_1 m (p q) + 2 c_4 m (p q) \\
&\quad 2 d_4 m (p q) \quad 2 d_5 m (p q) \quad 2 e_5 m (p q) \quad 4 f_5 m (p q) + \\
&\quad \frac{1}{2} F_a \quad 6 a_4 m + 8 a_5 m \quad b_{13} m + 8 b_5 m \quad 4 b_4 m^3 \\
&\quad 2 c_4 m^3 + c_5 m^3 \quad 2 d_4 m^3 + d_5 m^3 + 3 e_5 m^3 + 3 f_5 m^3 + \\
&\quad 2 a_1 m (p_K p) \quad 2 c_4 m (p_K p) + 2 d_4 m (p_K p) + 2 d_5 m (p_K p) + \\
&\quad 2 e_5 m (p_K p) + 4 f_5 m (p_K p) \quad 2 c_4 m (p_K q) + 2 d_5 m (p_K q) + \\
&\quad 2 f_5 m (p_K q) \quad \frac{3 a_{13} m}{(p q)} \quad \frac{b_{13} m^3}{2 (p q)} \quad \frac{b_{13} m (p_K p)}{(p q)} \\
&\quad \frac{b_{13} m (p_K q)}{(p q)} \quad 6 b_4 m (p q) \quad 4 c_4 m (p q) \quad 2 d_4 m (p q) + \\
&\quad 2 d_5 m (p q) + 2 e_5 m (p q) + 4 f_5 m (p q)
\end{aligned}$$

$$\begin{aligned}
\operatorname{Im} F_v &= \frac{1}{2} f_k - a_2 m^2 + c_3 m^2 + e_3 m^2 + \\
&\quad \frac{a_1 m^2}{(p \cdot q)} + \frac{b_1 m^2}{(p \cdot q)} - \frac{2 b_4 m^2}{(p \cdot q)} - \frac{c_4 m^2}{(p \cdot q)} - \frac{d_4 m^2}{(p \cdot q)} + \\
&\quad \frac{1}{2} F_a (6 a_4 - 2 a_5 - 8 b_5 + c_4 m^2 - d_4 m^2 - d_5 m^2 - e_5 m^2 \\
&\quad - 2 f_5 m^2 - 2 a_1 (p_k p) + 4 b_4 (p_k p) + 4 c_4 (p_k p) - 2 d_5 (p_k p) \\
&\quad - 2 e_5 (p_k p) - 4 f_5 (p_k p) - 2 a_1 (p_k q) + 2 b_4 (p_k q) + 4 c_4 (p_k q) \\
&\quad - 2 d_5 (p_k q) - 2 f_5 (p_k q) + 2 c_4 (p \cdot q) - 2 d_5 (p \cdot q) - 2 f_5 (p \cdot q) + \\
&\quad \frac{1}{2} F_v (-8 a_4 + 4 a_5 + 4 b_5 + 2 a_1 m^2 - 4 b_4 m^2 - 3 c_4 m^2 + c_5 m^2 \\
&\quad - d_4 m^2 - d_5 m^2 + 3 e_5 m^2 + 3 f_5 m^2 - 2 a_1 (p_k p) + 4 b_4 (p_k p) + \\
&\quad 4 c_4 (p_k p) - 2 d_5 (p_k p) - 2 e_5 (p_k p) - 4 f_5 (p_k p) - 2 a_1 (p_k q) + \\
&\quad 2 b_4 (p_k q) + 4 c_4 (p_k q) - 2 d_5 (p_k q) - 2 f_5 (p_k q) + 4 a_1 (p \cdot q) \\
&\quad - 6 b_4 (p \cdot q) - 6 c_4 (p \cdot q) + 2 d_5 (p \cdot q) + 2 e_5 (p \cdot q) + 4 f_5 (p \cdot q))
\end{aligned}$$

Figure captions

- 1. Feynman diagrams for the $K \rightarrow \pi \pi$ decay in the tree level of SM.
- 2. Feynman diagrams contributing to the muon transverse polarization in the tree level approximation of SM.
- 3. Bounds for the three doublets Weinberg model parameters coming from:) the analog of the KM matrix for the charged-Higgs boson mixings. The allowed parameter region is below the bounding curve;) the data on charged-Higgs search at LEP II (allowed region above the dashed line) and data on the $D^0 \bar{D}^0$ mixing (allowed region is above the solid line);) the data on the neutron EDM (allowed region is below the bounding curve).
- 4. The 3D Dalitz plot for the muon transverse polarization as a function of $x = 2E = m_K$ and $y = 2E = m_K$ for the one-loop approximation of SM.
- 5. Level lines for the Dalitz plot of the muon transverse polarization $P_T = f(x; y)$ in the SM case.
- 6. The 3D Dalitz plot for the muon transverse polarization as a function of $x = 2E = m_K$ and $y = 2E = m_K$ within the three doublets Weinberg model.
- 7. Level lines for the Dalitz plot of the muon transverse polarization $P_T = f(x; y)$ in the Weinberg model case.

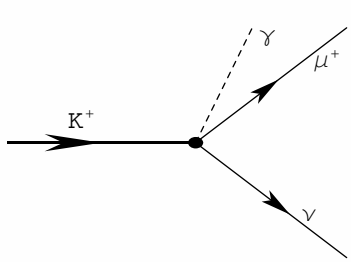


Fig. 1a

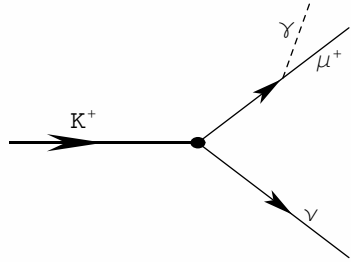


Fig. 1b

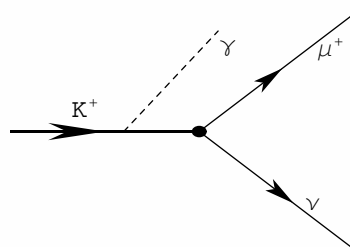


Fig. 1c

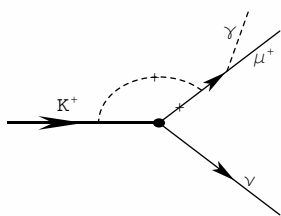


Fig. 2a

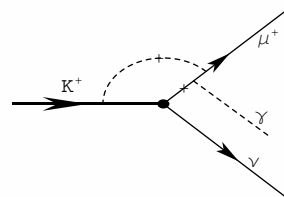


Fig. 2b

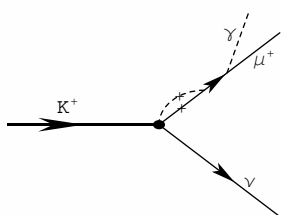


Fig. 2c

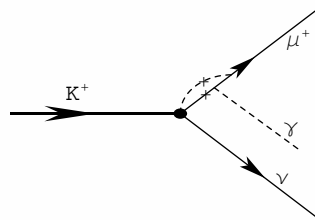


Fig. 2d

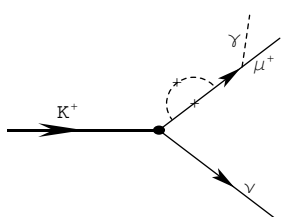


Fig. 2e

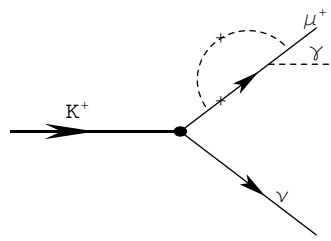


Fig. 2f

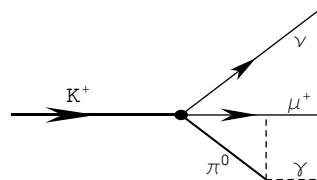


Fig. 2g

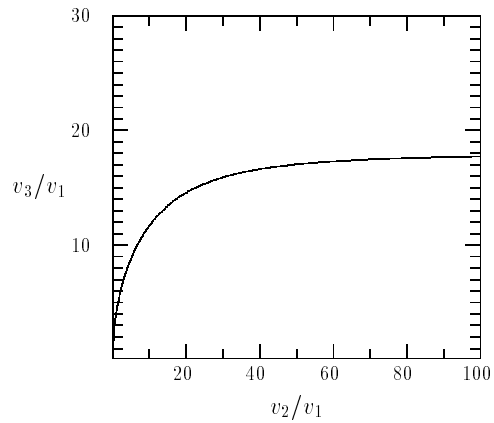


Fig. 3a

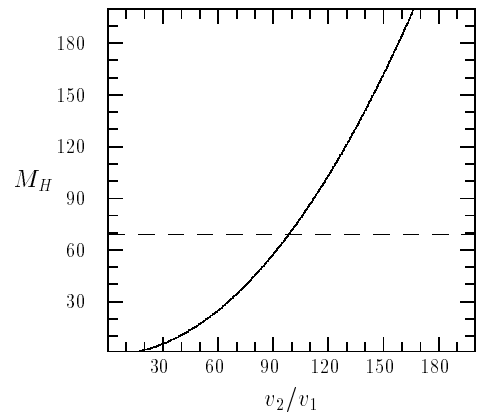


Fig. 3b

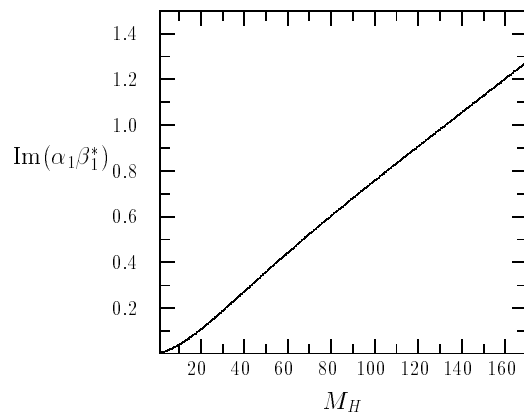


Fig. 3c

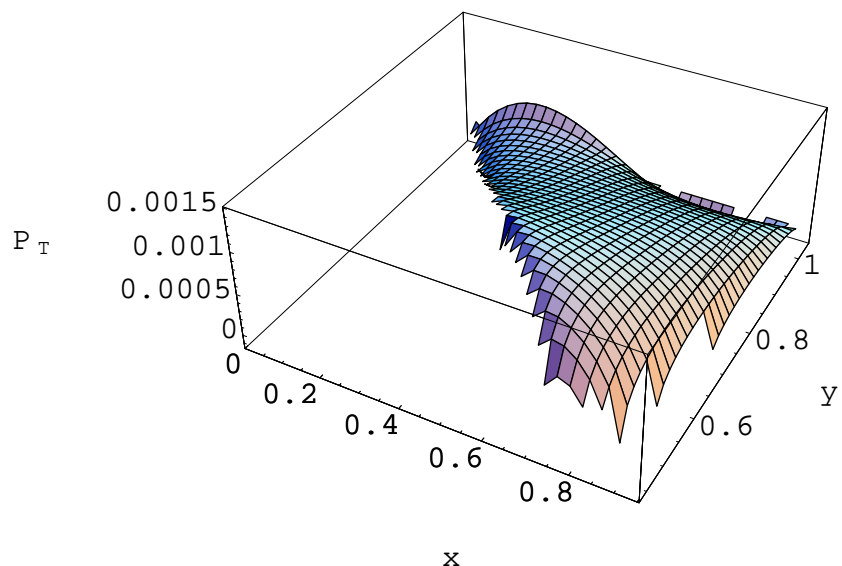


Fig. 4

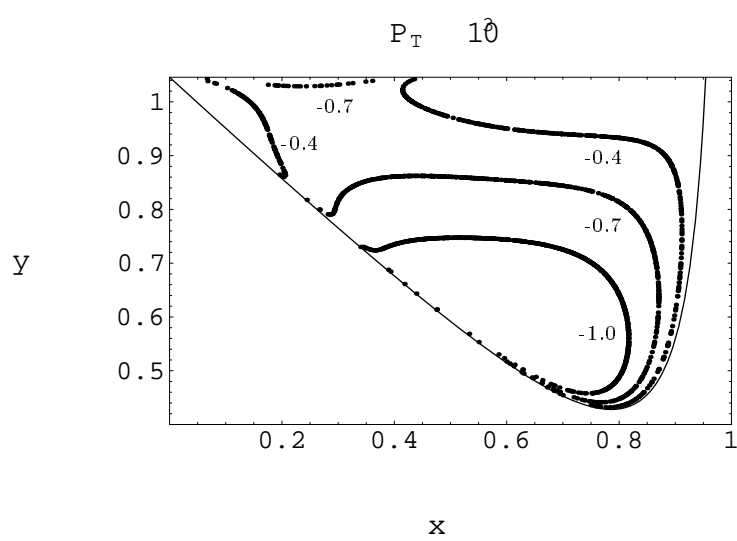


Fig. 5

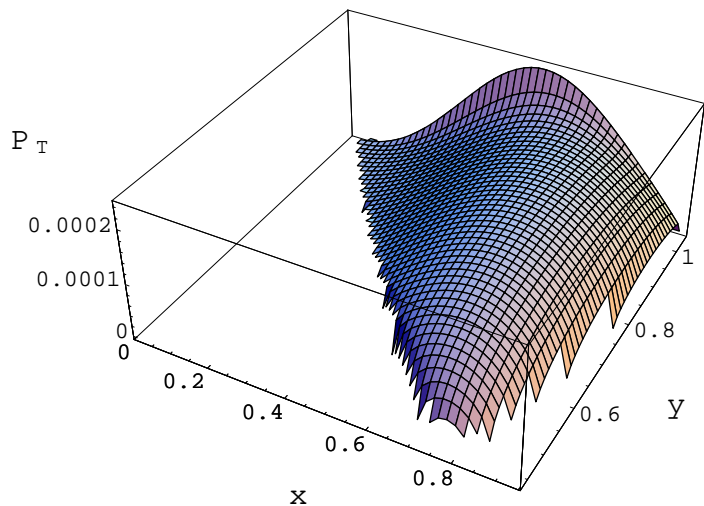


Fig. 6

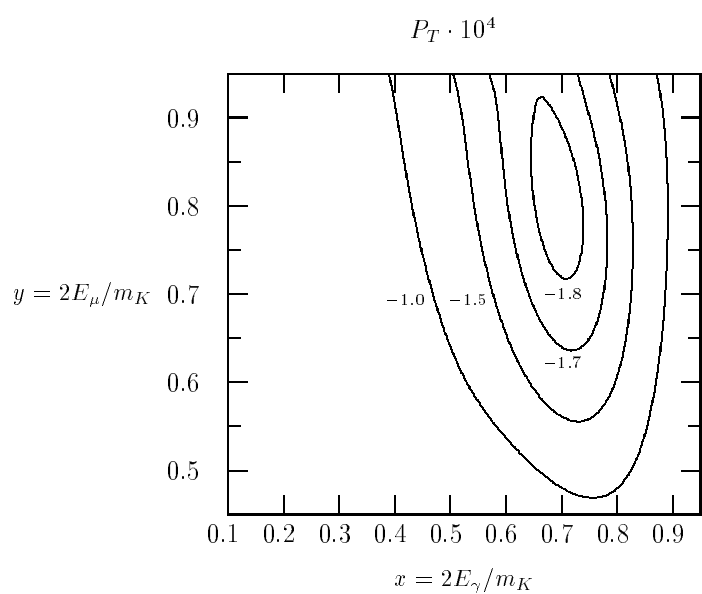


Fig. 7